ARTICLES
PUBLISHED ONLINE: 30 MAY 2016 | DOI: 10.1038/NNANO.2016.88
nature nanotechnology

Metal nanoparticles in the presence of lipopolysaccharides trigger the onset of metal allergy in mice

Toshiro Hirai[1], Yasuo Yoshioka[1,2,3]*, Natsumi Izumi[1], Ko-ichi Ichihashi[1], Takayuki Handa[1], Nobuo Nishijima[1], Eiichiro Uemura[1], Ko-ichi Sagami[1], Hideki Takahashi[1,2], Manami Yamaguchi[1], Kazuya Nagano[4], Yohei Mukai[5], Haruhiko Kamada[4,6], Shin-ichi Tsunoda[4,6], Ken J. Ishii[7,8], Kazuma Higashisaka[1] and Yasuo Tsutsumi[1,5,6]*

Many people suffer from metal allergy, and the recently demonstrated presence of naturally occurring metal nanoparticles in our environment could present a new candidate for inducing metal allergy. Here, we show that mice pretreated with silver nanoparticles (nAg) and lipopolysaccharides, but not with the silver ions that are thought to cause allergies, developed allergic inflammation in response to the silver. nAg-induced acquired immune responses depended on $CD4^+$ T cells and elicited IL-17A-mediated inflammation, similar to that observed in human metal allergy. Nickel nanoparticles also caused sensitization in the mice, whereas gold and silica nanoparticles, which are minimally ionizable, did not. Quantitative analysis of the silver distribution suggested that small nAg (≤10 nm) transferred to the draining lymph node and released ions more readily than large nAg (>10 nm). These results suggest that metal nanoparticles served as ion carriers to enable metal sensitization. Our data demonstrate a potentially new trigger for metal allergy.

Metal allergy, which is a type of allergic contact dermatitis, is prevalent in the general population. Nickel allergy is more prevalent than any other metal allergy, and it has been estimated that up to 17% of women and 3% of men are allergic to nickel[1,2]. In addition, gold, palladium, cobalt, mercury, beryllium, chromium, silver and other metals also have sensitization potential[3]. Costume jewellery, clothing fasteners (for example, buttons, zippers and belt buckles) and mobile phones are familiar sources of metal allergens[2,4].

Understanding metal allergy has been hindered by a lack of reproducible mouse models for studying the condition[5]. Although metal allergy is caused by metal-ion-induced T cells[6,7], many attempts to sensitize mice by means of simple metal-ion treatment have failed[8,9]. Recently, nickel ions (Ni^{2+}) were observed to directly activate Toll-like receptor 4 (TLR4) and to induce proinflammatory signals in humans, but not in mice[10]. Because some reports indicate that metal allergy in mice could be induced by coincident application of inflammatory stimuli, such as lipopolysaccharides (LPS)[11,12], a lack of proinflammatory signals in mice was presumed to sufficiently explain why they do not develop metal allergy through the simple introduction of metal ions. However, another report argued that skin reactions in those models were induced by irritant inflammations rather than by allergic responses[13], which calls into question the reproducibility of those mouse models. These findings also suggest that another, unknown factor might induce the onset of metal allergy.

Metal nanoparticles have been known to be generated not only by laboratory synthesis, but also naturally (or unintentionally) during our daily lives[14]. For example, metal-on-metal implants for joint replacement are known to produce nanoscale debris in the human body[15,16], and patients with failed joint replacements have been observed to exhibit metal allergy at a high prevalence[17]. Earrings and metal wires have been observed to release naturally occurring metal nanoparticles in a laboratory environment[18], and recent data have shown that nanoparticles can penetrate damaged and intact skin, as metal ions do[19,20]. These observations suggest that metal nanoparticles are a new candidate for causing metal allergy. In this study, we investigated the role of metal nanoparticles in inducing metal allergy in mice. Our data suggest that metal nanoparticles are a new potential trigger of metal allergy.

nAg sensitize mice and cause allergic inflammation

We used silver nanoparticles (nAg) with diameters of 10, 50 and 100 nm (nAg10, nAg50 and nAg100, respectively). Their hydrodynamic diameters in isotonic glucose (5%) were 19.4, 55.2 and 107.3 nm, respectively (Supplementary Fig. 1a), indicating that they are well-dispersed in solution. Transmission electron microscopy (TEM) images confirmed that the nanoparticles were uniform in size

[1]Laboratory of Toxicology and Safety Science, Graduate School of Pharmaceutical Sciences, Osaka University, 1-6 Yamadaoka, Suita, Osaka 565-0871, Japan. [2]Vaccine Creation Project, BIKEN Innovative Vaccine Research Alliance Laboratories, Research Institute for Microbial Diseases, Osaka University, 3-1 Yamadaoka, Suita, Osaka 565-0871, Japan. [3]BIKEN Center for Innovative Vaccine Research and Development, The Research Foundation for Microbial Diseases of Osaka University, 3-1 Yamadaoka, Suita, Osaka 565-0871, Japan. [4]Laboratory of Biopharmaceutical Research, National Institutes of Biomedical Innovation, Health and Nutrition, 7-6-8 Saitoasagi, Ibaraki, Osaka 567-0085, Japan. [5]Laboratory of Innovative Antibody Engineering and Design, Center for Drug Innovation and Screening, National Institutes of Biomedical Innovation, Health and Nutrition, 7-6-8 Saitoasagi, Ibaraki, Osaka 567-0085, Japan. [6]The Center for Advanced Medical Engineering and Informatics, Osaka University, 1-6 Yamadaoka, Suita, Osaka 565-0871, Japan. [7]Laboratory of Adjuvant Innovation, National Institutes of Biomedical Innovation, Health and Nutrition, 7-6-8 Saitoasagi, Ibaraki, Osaka 567-0085, Japan. [8]Laboratory of Vaccine Science, Immunology Frontier Research Center, World Premier International Research Center, Osaka University, 3-1 Suita, Osaka 565-0871, Japan.
*e-mail: y-yoshioka@biken.osaka-u.ac.jp; ytsutsumi@phs.osaka-u.ac.jp

(Supplementary Fig. 1b). The silver ion (Ag^+) contents in nAg10, nAg50 and nAg100 solutions were confirmed to be ~7.5, 2.5 and 2.0%, respectively (Supplementary Table 1). Inflammatory potential increased with decreasing particle size (Supplementary Fig. 2a).

We injected nAg10 or Ag^+ into each BALB/c mouse's footpads together with LPS. One week after the last treatment, nAg10 or Ag^+ was administered to the ear of each mouse. Ear swelling was measured to evaluate the elicitation of a metal-specific allergic response. In addition, the amount of Ag^+ administered to the ear was about one-ninth the amount of administered nAg10, because the induced inflammation was so strong that the analytical signal was saturated at higher doses of Ag^+ (Supplementary Fig. 2a,b). Ag^+ pretreatment did not induce significant changes in either Ag^+- or nAg10-induced ear swelling (Fig. 1a). In contrast, mice that were pretreated with nAg10 developed significant ear swelling following administration of both Ag^+ and nAg10. Histological observations also showed that the inflammation in nAg10- and Ag^+-treated ears was significantly enhanced by nAg10 pretreatment (Fig. 1b,c). In addition, the enhancement effect of nAg was specific to silver rather than to the vehicle (Supplementary Fig. 2c). It is well known that nAg can release Ag^+ (ref. 21). Thus, we consider these results to at least reflect a nAg10-induced Ag^+-specific immune response, and they might also indicate a nAg-induced nAg-specific immune response.

BALB/c mice sensitized with nAg10 without LPS and with an underacylated form of *Rhodobacter sphaeroides* LPS (LPSa, which does not induce TLR4-mediated proinflammatory signals) did not display nAg10-induced sensitization (Fig. 1d). In contrast, ultrapure LPS was sufficient to induce the enhancement (Supplementary Fig. 2d). Thus, a proinflammatory signal, specifically a TLR4 signal, was needed to observe nAg10-induced sensitization. Therefore, although Ag^+ could not cause sensitization, our data are partially consistent with reports that suggest the necessity of an additional proinflammatory signal to cause sensitization to metal in mice[11,12]. In addition, nAg10 could cause sensitization in C57BL/6 mice, but the effect in these mice seemed to be weaker than that observed in BALB/c mice (Supplementary Fig. 2e).

The nAg10 pretreatment enhanced not only nAg10-induced ear swelling, but also nAg50- and nAg100-induced swelling (Fig. 1e). nAg50 sensitization also tended to enhance nAg10-induced ear swelling. Furthermore, we confirmed that pretreatment with nAg with diameters of 5 nm (nAg5) enhanced nAg5- or nAg10-induced ear swelling significantly (Supplementary Fig. 3). Taken together, these results suggest that the size of the sensitizing nAg does not have to match that of the administered nAg to observe nAg-induced ear swelling, which suggests that nAg did not induce nanoparticle-specific immune responses. However, it should be noted that smaller nAg appeared to have a stronger sensitization potential and ability to induce a more pronounced inflammatory response in nAg-sensitized BALB/c mice.

Involvement of acquired immunity in sensitization by nAg10

Metal allergy is an allergic contact dermatitis, which is induced by acquired immunity involving T, B and NK cells[22–24]. To determine whether the effect of sensitization with nAg is an antigen-specific acquired immune response, we compared the effect of sensitization by nAg10 on nAg10-induced ear swelling among BALB/c, nude possessing few T cells, and T cell- and B cell-deficient severe combined immunodeficient (SCID) mice. nAg10 could cause sensitization in nude mice, although the enhancement of nAg10-induced ear swelling seemed to be weaker than that observed for BALB/c mice (Fig. 2a). No sensitization by nAg10 was observed in SCID mice. These results suggest that nAg10 sensitization is associated with an acquired immune response.

Treatment with $CD4^+$ T cell-depleting antibodies (anti-CD4) 24 h before injection of nAg10 to each mouse's ear completely suppressed nAg10-induced ear swelling, but $CD8^+$ T cell- or NK cell-depleting antibodies (anti-CD8 and anti-asialo GM1, respectively) did not induce detectable effects (Fig. 2b). Furthermore, adaptive transfer of $CD4^+$ T cells from nAg10-sensitized BALB/c mice enhanced nAg10-induced ear swelling (Fig. 2c). In contrast, adoptive transfer of the serum from nAg10-sensitized BALB/c mice did not substitute for pretreatment with nAg (Fig. 2c), and little enhancement of nAg10-induced ear swelling was induced by nAg10 sensitization at early time points (0.25–6 h) post-injection (Supplementary Fig. 2f). Therefore, $CD4^+$ T cells, but not the antibodies, appeared to play a critical role in nAg10-induced allergic responses.

The splenocytes from nAg10-sensitized BALB/c mice were stimulated by each size of nAg or by Ag^+. We evaluated the production of several T cell-mediated cytokines: IFN-γ as a Th1-related cytokine, IL-4 and IL-5 as Th2-related cytokines, IL-9 as a Th9-related cytokine and IL-17A as a Th17-related cytokine in the splenocyte culture supernatants. Neither nAg10 nor Ag^+ stimulation induced detectable changes in IFN-γ, IL-4, IL-5 or IL-9 levels for vehicle-sensitized and nAg10-sensitized splenocytes (Supplementary Fig. 4). In contrast, IL-17A production was more pronounced following nAg10 or Ag^+ stimulation in nAg10-sensitized splenocytes than in vehicle-sensitized splenocytes (Fig. 3a). Thus, nAg10 sensitization could induce Th17-mediated immune responses. nAg10-sensitized splenocytes stimulated with nAg50 or nAg100 induced IL-17A, but the amount was lower than when the splenocytes were stimulated with nAg10 (Fig. 3a). These tendencies are similar to the results observed *in vivo* (Fig. 1e). Furthermore, other types of metal nanoparticles (for example, nickel) did not induce IL-17A production (Fig. 3b). Considering the fact that a decrease in particle size enhances Ag^+ release per mass (Supplementary Table 1), we concluded that the majority of nAg-induced immunity could be attributed to Ag^+-specific immune responses.

Higher expression of *Il17a* in nAg10-injected ears was also observed *in vivo* in nAg10-sensitized BALB/c mice when compared to vehicle-sensitized BALB/c mice (Fig. 3c). Furthermore, although treatment with IFN-γ-neutralizing antibody had no significant effect on the enhancement of nAg10-induced ear swelling, treatment with IL-17A-neutralizing antibody partially but significantly suppressed the swelling (Fig. 3d). Considering the importance of $CD4^+$ T cells in nAg10-induced allergic responses, Th17 could be one of the major effector cells in our model.

Lymphatic transport of nAg

After antigens enter the body through the skin or by other means, they flow through afferent lymphatics into the draining lymph node (dLN) directly (conduit system) or after being captured by peripheral dendritic cells[25,26]. The initial activation of naive T cells and induction of antigen-specific T cells occur sequentially in the dLN[27] and thus the rate of antigen transfer or retention in the dLN might have influenced whether the mice were sensitized to the antigen. We quantitatively compared the distributions of each size of nAg with the distribution of Ag^+ in the dLN of the injected ear. Higher amounts of Ag were detected in the dLN for all nAg-treated groups than for the Ag^+ group at 24, 48 and 96 h (Fig. 4a). nAg10 was consistently present at significantly higher levels than the larger nAg. These size effects were consistent with other previously reported results[28,29].

TEM observations revealed that several antigen-presenting cells (APCs) seemed to take up nAg10 in nAg10-treated BALB/c mice in the dLN, although we could not find nAg in the dLN of the nAg50- or nAg100-treated groups (Fig. 4b). Thus, sensitizing nAg10 was probably transported to the dLN as nanoparticles rather than as ions that were disassociated from nanoparticles in the dermis. On the other hand, a significant and time-dependent decrease in the amount of Ag in the dLN was observed when

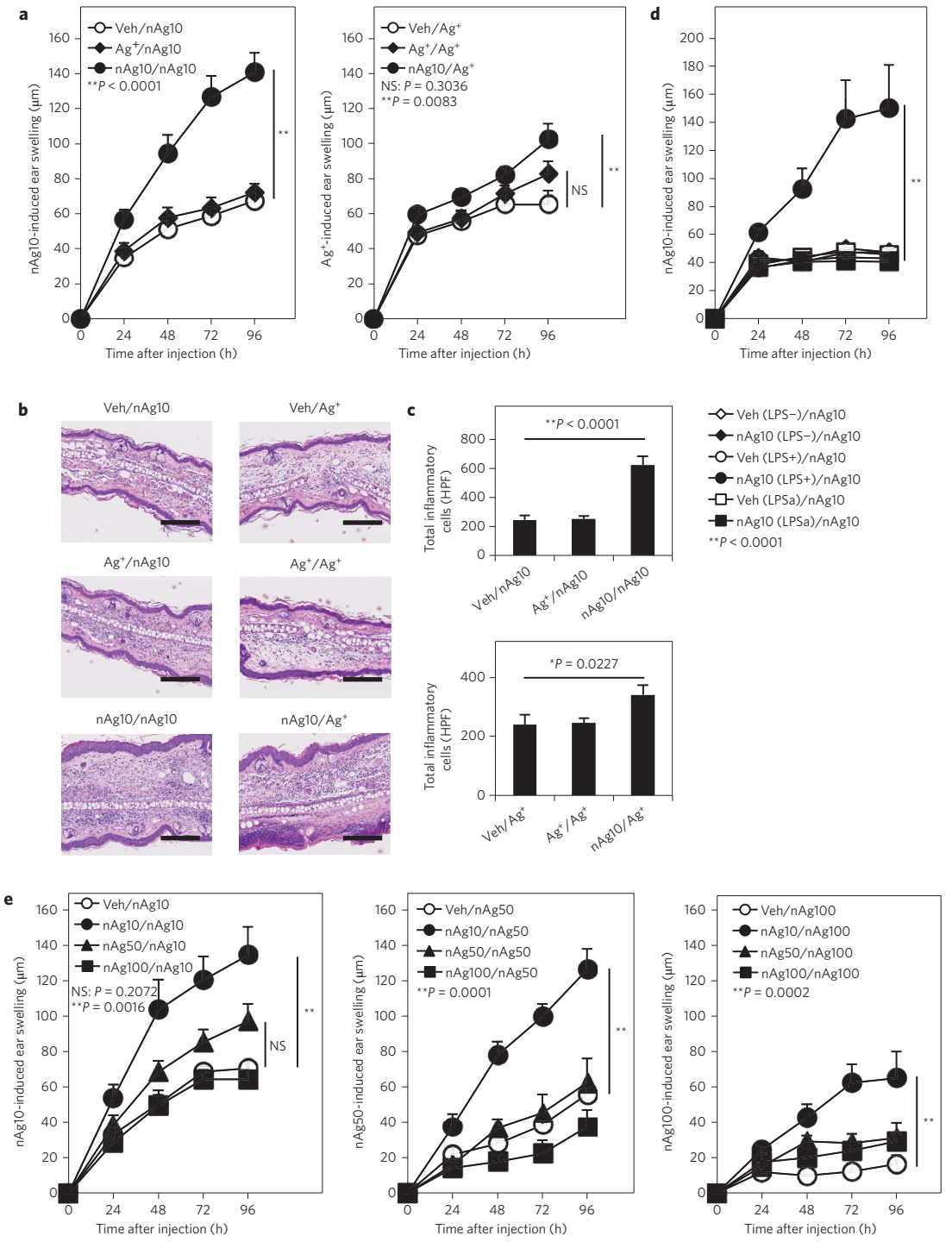

Figure 1 | Sensitization potential of silver nanoparticles. a, Comparison of the effect of pretreatment with nAg10 or Ag^+ on nAg10- (left) and Ag^+-induced (right) ear swelling in BALB/c mice. Pretreatment with nAg10 and lipopolysaccharides (LPS), but not with Ag^+, induced more severe inflammation in response to nAg10 or Ag^+ challenge. Left: $n = 12$ (open circles), 10 (filled diamonds) and 12 (filled circles) mice per group. Right: $n = 10$ mice per group. **b**, Representative images of ear sections stained with haematoxylin and eosin 96 h after administration of nAg10 or Ag^+ in nAg10- or Ag^+-pretreated BALB/c mice, showing that the nAg10-pretreatment induced more severe ear swelling and infiltration of inflammatory cells in response to nAg10 or Ag^+. Scale bars, 200 μm. **c**, Total inflammatory cell infiltration per high-power field (HPF) in the stained sections. Upper panel, left to right: $n = 5$, 5 and 6 sections per group. Lower panel, left to right: $n = 6$, 5 and 6 sections per group. Each section was obtained from different BALB/c mice. **d**, Effects of LPS on sensitization potential of nAg10 in BALB/c mice: $n = 4$ (open diamonds), 4 (filled diamonds), 5 (open circles), 4 (filled circles), 3 (open squares) and 3 (filled squares) mice per group, respectively. LPS was required for nAg10 to cause sensitization. **e**, Effects of nAg size on sensitization potential in BALB/c mice. Smaller nAg appeared to have a stronger sensitization potential. Left: $n = 5$ (open circles), 6 (filled circles), 6 (filled triangles) and 6 (filled squares) mice per group, respectively. Centre: $n = 6$ (open circles), 5 (filled circles), 6 (filled triangles) and 5 (filled squares) mice per group, respectively. Right: $n = 5$ (open circles), 4 (filled circles), 6 (filled triangles) and 6 (filled squares) mice per group, respectively. Each experiment was performed twice (**b**–**d**), three times (**e**) or four times (**a**). Data are means ± s.e.m. $*P < 0.05$, $**P < 0.01$ versus the vehicle-sensitized group (Dunnett's test). The labels used in the figure legends are listed in the order of 'pretreatment sample'/'administered sample'. Veh, vehicle; NS, not significant.

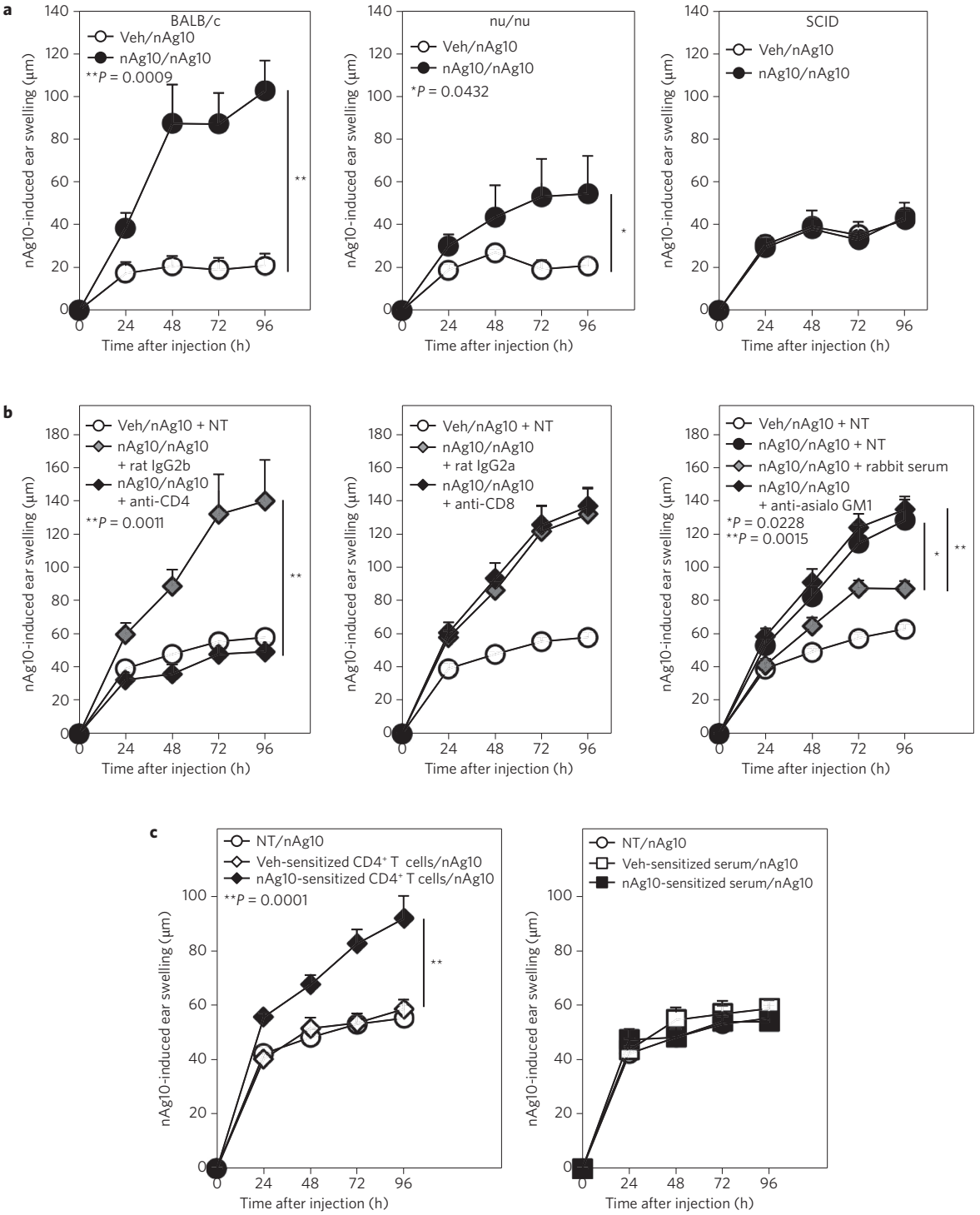

Figure 2 | Relationship between acquired immunity and the effects of nAg10 pretreatment. a, Sensitization potential of nAg10 in BALB/c mice, in nude mice possessing few T cells and in T cell- and B cell-deficient SCID mice. nAg10 pretreatment had the greatest effect in BALB/c mice, suggesting that nAg10 elicited acquired immunity to silver. Left: $n = 5$ (open circles) and 6 (filled circles) mice per group, respectively. Centre: $n = 6$ (open circles) and 5 (filled circles) mice per group, respectively. Right: $n = 5$ (open circles) and 4 (filled circles) mice per group, respectively. **b**, Effect of depletion of $CD4^+$, $CD8^+$ and NK cells on inflammatory response to nAg10 in nAg10-sensitized BALB/c mice treated with the depletion antibodies anti-CD4 (left), anti-CD8 (centre) and anti-asialo GM1 (right) or their isotype control rat IgG2b (left), rat IgG2a (centre) and rabbit serum (right). Left: $n = 5$ (open circles), 4 (grey diamonds) and 4 (black diamonds) mice per group, respectively. Centre: $n = 5$ (open circles), 3 (grey diamonds) and 5 (black diamonds) mice per group, respectively. Right: $n = 13$ (open circles), 9 (filled circles), 8 (grey diamonds) and 16 (black diamonds) mice per group, respectively. **c**, Effects of adaptive transfer of nAg10-sensitized $CD4^+$ T cells or serum on nAg10-induced ear swelling in BALB/c mice, confirming that nAg10 induced a $CD4^+$ T cell-dependent allergic response. Left: $n = 6$ (open circles), 4 (open diamonds) and 4 (filled diamonds) mice per group, respectively. Right: $n = 6$ (open circles), 5 (open squares) and 5 (filled squares) mice per group, respectively. Each experiment was performed twice. Data are means ± s.e.m. $*P < 0.05$, $**P < 0.01$ versus control group (Dunnett's test). The labels used in the figure legends are listed in the order of 'pretreatment sample'/'administered sample' or 'pretreatment sample'/'administered sample' + 'antibody treatment'. Veh, vehicle; NT, not treated.

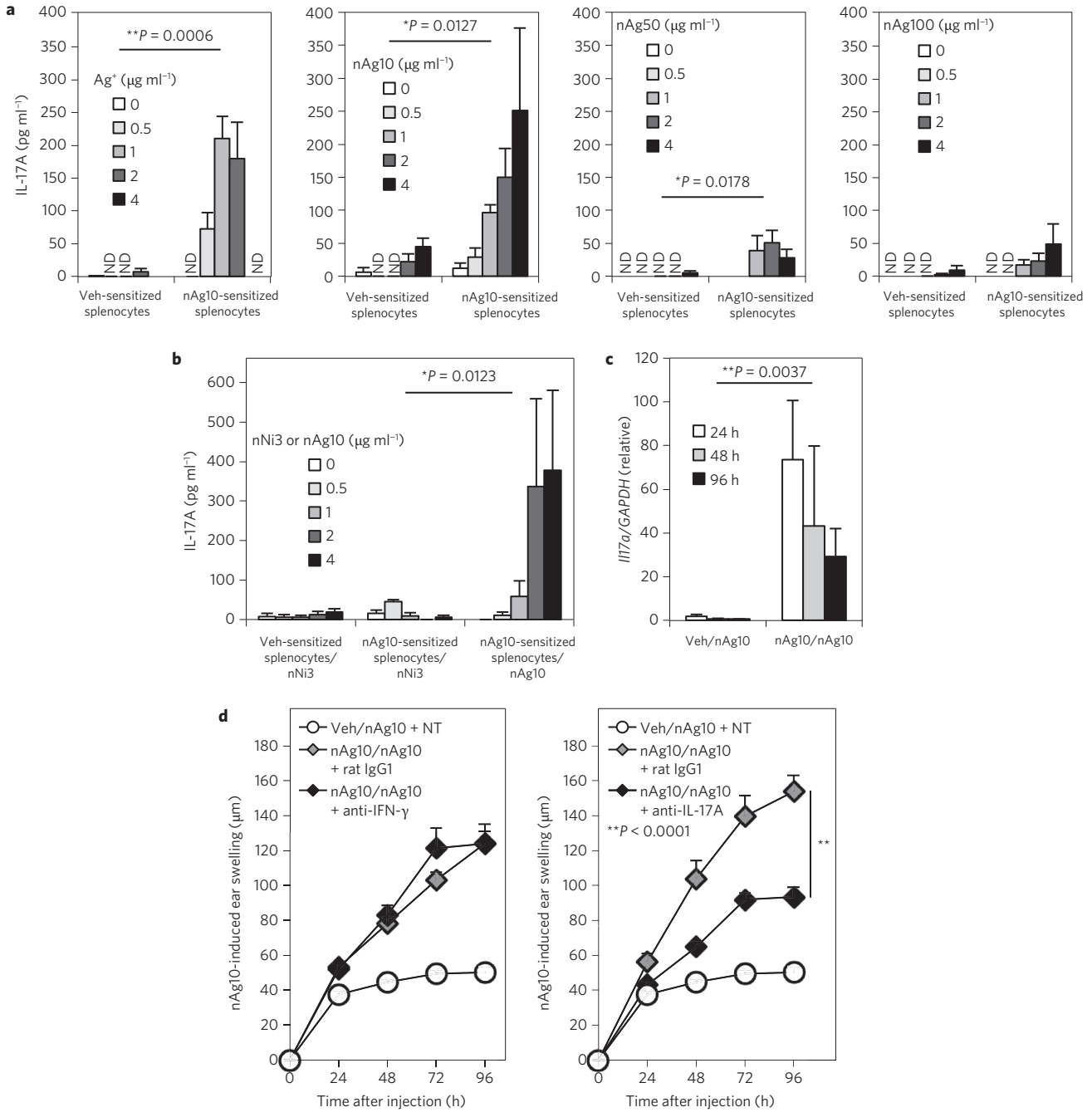

Figure 3 | Effector response induced by nAg10 sensitization. a,**b**, Levels of IL-17A in the supernatants of splenocytes from nAg10-sensitized BALB/c mice after stimulation with relevant antigen (each size of nAg or Ag^+) (**a**, $n = 6$ separate cultures of splenocytes per group) or irrelevant antigen (nNi3) (**b**, $n = 5$ separate cultures of splenocytes per group) for 72 h, as determined by enzyme-linked immunosorbent assay. Splenocytes from nAg10-sensitized mice produced IL-17A in response to nAg and Ag^+. Each culture was prepared from different mice. **c**, Relative amounts of *Il17a* transcript in nAg10-injected ear determined by quantitative PCR and normalized to *GAPDH*. nAg10-sensitized BALB/c mice induced higher *Il17a* expression in response to nAg10 than Veh-sensitized mice. $n = 4$ (open squares), 4 (grey squares) and 4 (black squares) mice, respectively, in the Veh/nAg10 group and $n = 5$ (open squares), 4 (grey squares) and 4 (black squares) mice, respectively, in the nAg10/nAg10 group. **d**, Effect of blockades of IFN-γ and IL-17A by neutralizing antibodies (anti-IFN-γ and anti-IL-17A, respectively) on nAg10-induced ear swelling in nAg10-sensitized BALB/c mice. Rat IgG1 was the isotype control for the neutralizing antibodies. The IL-17A blockade suppressed nAg10-induced ear swelling in the nAg10-sensitized BALB/c mice. Left: $n = 10$ (open circles), 7 (grey diamonds) and 8 (black diamonds) mice per group, respectively. Right: $n = 10$ (open circles), 8 (grey diamonds) and 9 (black diamonds) mice per group, respectively. Each experiment was performed twice (**b**–**d**) or seven times (**a**). Data are means ± s.e.m. $^*P < 0.05$, $^{**}P < 0.01$ versus control group (Dunnett's test). The labels used in the figure legends are listed in the order of 'pretreatment sample'/'administered sample or stimulated antigen' + 'antibody treatment'. Veh, vehicle; ND, not detected; NT, not treated.

nAg10, but not nAg50 or nAg100, was co-injected with LPS; similar kinetics were observed for the Ag^+ + LPS-treated group (Fig. 4a). nAg10 can release more ions than the larger nAg due to the higher particle number of nAg10 and also its larger surface area per mass (Supplementary Table 1). Therefore, the similarity in behaviour between nAg10 and Ag^+ in the dLN could mean that

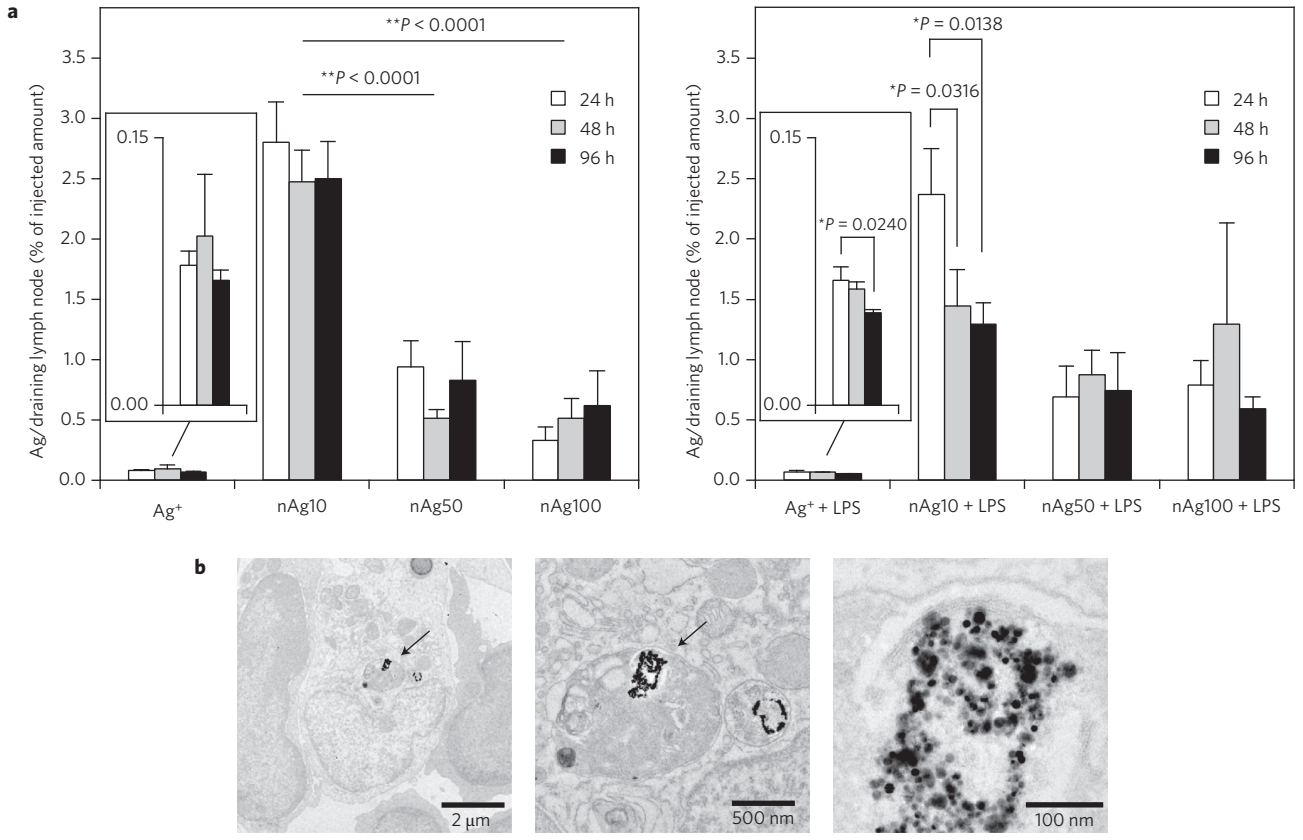

Figure 4 | Distribution of nAg in draining lymph node. a, Amounts of silver in draining lymph node of BALB/c mice were quantitatively determined by ICP-MS up to 96 h after intradermal injection at the ear with each size of nAg with/without LPS or with Ag^+. nAg10 transferred to the draining lymph node and released ions more readily than large nAg (>10 nm). Left: $n = 8$, 13, 13 and 13 mice per group for Ag^+, nAg10, nAg50 and nAg100, respectively. Right: $n = 5$, 13, 5 and 5 mice per group for Ag^+ + LPS, nAg10 + LPS, nAg50 + LPS and nAg100 + LPS, respectively. **b**, TEM images of draining lymph node of BALB/c mice 24 h after administration of nAg10 to the ear (three images display the same sample at three different magnifications). nAg10 was transported to the draining lymph node as nanoparticles rather than as ions that were disassociated from nanoparticles in the dermis. Arrows point to nAg10. Each experiment was performed twice (**b**) or three times (**a**). Data are means ± s.e.m. $^*P < 0.05$, $^{**}P < 0.01$ (Dunnett's test).

nAg10 released ions in the dLN after being transported there. Although the mechanism of Ag^+ excretion from the dLN by LPS is unknown, our results suggest that nAg10 can be transported to the dLN at a higher rate than Ag^+ or larger nAg and that nAg10 released ions in the dLN at a higher rate than larger nAg. Because nAg10 sensitization induced Ag^+-specific immune responses (Figs 1 and 3a), the combination of superior lymphatic transport and the generation of ions from nanoparticles appears to have been a critical determinant of the ability of nAg to cause sensitization in this study.

Universality of sensitization potentials of nanoparticles

We used nickel nanoparticles with a diameter of 3 nm and gold nanoparticles with a diameter of 10 nm (nNi3 and nAu10, respectively); both of these metals are known to be sensitizers for humans[3]. We also tested amorphous silica nanoparticles with a diameter of 10 nm (nSP10) as non-metal nanoparticles. TEM analysis showed that nAu10 and nSP10 were uniform and well-dispersed particles. In contrast, nNi3 formed aggregates/agglomerates, but some of the aggregates/agglomerates appeared to be small (≤10 nm) (Supplementary Fig. 1b). nNi3 pretreatment with LPS, but not Ni^{2+} or without LPS, caused sensitization to both nNi3 and Ni^{2+} (Fig. 5a–d and Supplementary Fig. 6). Thus nNi3, but not Ni^{2+}, had the ability to cause sensitization in our model. In contrast, neither nAu10 nor nSP10 could cause sensitization (Supplementary Fig. 5). Considering that gold is the most stable metal and that our nAu10 released few ions (Supplementary Table 1), we concluded that the differences among the abilities of the particles to release ions were related to the observed sensitization potentials. nNi3-sensitized splenocytes induced an IL-17A response, but not IFN-γ, IL-4 or IL-5 responses, to nNi3 and Ni^{2+} stimulation *in vitro* (Supplementary Fig. 7). These results were similar to the results for nAg-sensitized splenocytes (Fig. 3a).

nAg10 sensitization did not change nNi3-induced ear swelling, and nNi3 sensitization also caused no significant changes in nAg10-induced swelling (Fig. 5e). Although simultaneous sensitivity to several metals is a common clinical observation[30], the nAg10- and nNi3-induced immune responses were not cross-reactive to each other.

Particulate matter, including nanoparticles, has characteristic adjuvant effects on acquired immunity[31]. It is thus possible that the sensitization potential of nAg can be explained by an adjuvant effect of nAg on co-existing Ag^+. However, Ag^+ + LPS combined with nNi3 failed to cause sensitization to silver (Fig. 5f). We also evaluated the effect of nAg on LPS-induced inflammation. *Il6* and *TNFα* expression induced by LPS were not affected by co-administration of Ag^+ or any size of nAg (Supplementary Fig. 8). Together, the high sensitization potentials of metal nanoparticles observed here appear to be independent of the adjuvanticity of the particles. That could mean that the metal nanoparticles served as ion carriers rather than adjuvants.

The metal debris generated from metal-on-metal implants used for total hip replacement is estimated to produce 10^{12} to 10^{14} particles per year with an average particle size of less than 50 nm (refs 15,32). However, difficulties in isolating and characterizing small particles, particularly those smaller than 10 nm, could mean

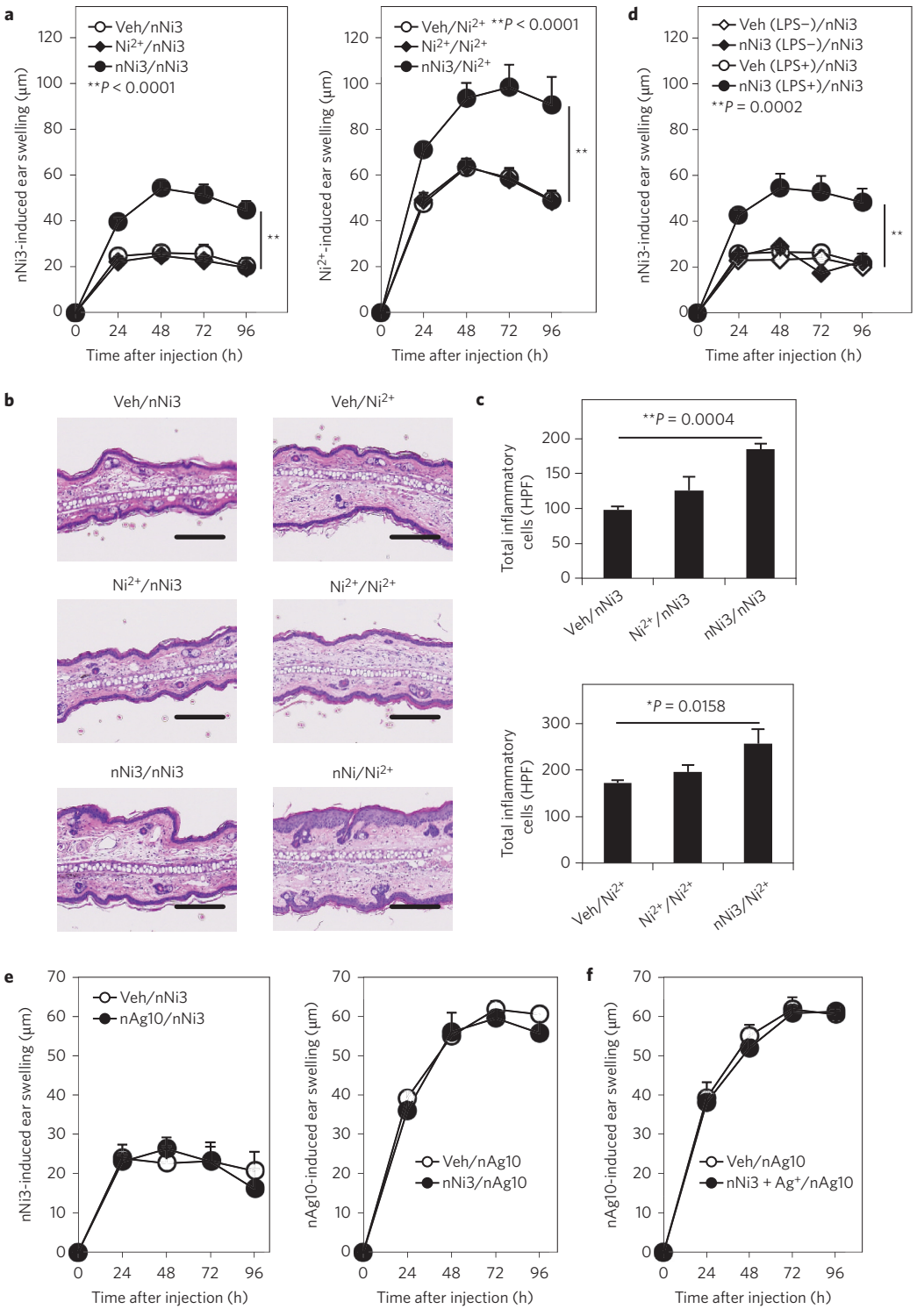

Figure 5 | Effect of nickel nanoparticles on nickel sensitization. a, Comparison of the effects of nNi3 and Ni^{2+} on sensitization to nickel in BALB/c mice. nNi3 with LPS, but not ions, induced nickel sensitization. Left panel: $n = 8$ (open circles), 9 (filled diamonds) and 10 (filled circles) mice per group, respectively. Right: $n = 10$ mice per group. **b**, Representative images of ear sections stained with haematoxylin and eosin 96 h after administration of nNi3 or Ni^{2+} in nNi3- or Ni^{2+}-sensitized BALB/c mice. The nNi3-pretreatment induced more severe ear swelling and infiltration of inflammatory cells in response to nNi3 or Ni^{2+}. Scale bars, 200 μm. **c**, Evaluation of total inflammatory cell infiltration per high-power field (HPF) in the stained sections. Upper panel, left to right: $n = 4$, 4 and 5 sections per group. Lower panel, $n = 4$ sections per group. Each section was obtained from different BALB/c mice. **d**, Effect of pretreatment with nNi3, with or without LPS, on nNi3-induced ear swelling in BALB/c mice: $n = 4$ (open diamonds), 5 (filled diamonds), 4 (open circles) and 5 (filled circles) mice per group, respectively. LPS was required for nNi3 to cause sensitization. **e**, Cross-reactivity of nAg10 sensitization to nNi3 allergic response (left) and nNi3 sensitization to nAg10 allergic response (right) in BALB/c mice: $n = 4$ mice per group. The nAg10- and nNi3-induced immune responses were not cross-reactive to each other. **f**, Adjuvant effect of nNi3 on Ag^{+} sensitization in BALB/c mice: $n = 4$ per group. Co-administration of nNi3 with Ag^{+} failed to elicit the allergic response to silver. Each experiment was performed twice. Data are means ± s.e.m. $^{*}P < 0.05$, $^{**}P < 0.01$ versus vehicle-sensitized group (Dunnett's test). The labels used in the figure legends are listed in the order of 'pretreatment sample'/'administered sample'. Veh, vehicle.

that the average size and the number of these nanoparticles are underestimated[15,32]. In the present study, we have shown that metal nanoparticles, particularly those 10 nm or smaller, cause sensitization. Considering that total hip and total knee replacements are projected to increase by 137 and 601%, respectively, between 2005 and 2030 (ref. 33), more information should be obtained regarding metal nanoparticles generated from implants.

Naturally occurring nanoparticles are thought to be formed from dissolved ions in metal objects[18]. These dissolved ions could first interact with organic or inorganic chelate ligands existing on the skin or other exterior surfaces of the human body. Generation of metal nanoparticles has been observed in natural river waters under sunlight[34] and in a biological fluidic model[35], both of which contained organic and inorganic chelate ligands. Furthermore, nAg has been observed to form *in vivo* after oral Ag^+ treatment of rats[36]. These previous reports all indicate that nanoparticles occur naturally in physiological environments and that they can be introduced into a living body by cutaneous exposure to metal objects. Therefore, the contribution of intermediate nanoparticle phases to the onset of metal allergy should be assessed in humans in future studies.

The recognition of chemical sensitizers by pattern-recognition receptors has been revealed to be crucial to the elicitation of acquired immune responses, which subsequently induce allergic contact dermatitis[37]. In particular, nickel, cobalt and palladium ions are reported to be recognized by human TLR4 (refs 10,38). Because metal nanoparticles can form from ions and can also release ions under physiological conditions, metal nanoparticles present in the human body are most probably always accompanied by metal ions. Thus, adjuvants such as LPS might not be needed for sensitization in humans. However, because a metal-ion-mediated signal via TLR4 is expected to differ from a CD14-required, LPS-mediated signal[39], metal ions might not serve as a direct substitute for LPS for metal sensitization in humans. Because the surface of the human body is not sterile, any naturally occurring nanoparticles on the body surface are likely to coexist there with bacterial adjuvants such as LPS. Furthermore, inside the human body, the same pattern-recognition receptors activated by bacteria can also be activated by non-microbial signals (that is, danger-associated molecular patterns)[40]. Further studies are needed to determine whether our treatment, that is, metal nanoparticles with LPS, could indeed cause metal allergy in humans.

Our data conflict with data reported by Sato *et al.*[12], but are consistent with those of Johansen and co-workers[13]. Sato *et al.* argued that nickel and silver ions combined with LPS cause sensitization in mice, whereas Johansen *et al.* suggest that these models are independent of allergic inflammation. Accumulated data, including our own, have shown that even at a maximum dosage, metal ions are too weak to be effective sensitizers and thus variations in preparation conditions or experimental environmental factors might affect the results. Meanwhile, metal nanoparticles could be generated from metal ions, as mentioned above. Therefore, another possible explanation of the conflict among the previous reports might be that experimental conditions affect the generation of naturally occurring nanoparticles.

It has been suggested that $CD4^+$ T cells contribute more than $CD8^+$ T cells in nickel allergy[41,42]. $IL\text{-}17^+$ T cells have also been reported to have a major pathogenic role in nickel allergy, although IFN-γ was thought to also contribute to the pathology[41]. In our model, the silver-induced allergic response was dependent on $CD4^+$ T cells (Fig. 2b,c) and IL-17A, but not on IFN-γ (Fig. 3a–d). Although the differentiation of Th1 and Th17 cells is mutually exclusive in mice, human T cells have plasticity. Furthermore, human T cells, but not mouse T cells, can co-release IFN-γ and IL-17 (ref. 43). Taken together, these species' differences with regard to T cells would give rise to differences between our models and human metal allergy.

We could not detect significant sensitization or a decrease in Ag in the dLN after nAg50 or nAg100 + LPS treatment (Fig. 1e and Fig. 4a). Antigen size can determine the efficiency of uptake by the dLN, as well as uptake and processing by APCs; these synergistic effects regulate the immune response[44]. Although a weak ability to cause sensitization is attributed to poor release of ions (Supplementary Table 1) and poor efficiency of uptake to the dLN (Fig. 4a), further study is needed to elucidate whether the ability of small nanoparticles to cause sensitization was affected by differences in APC kinetics.

Airborne particulates containing sensitizer metals can contribute to the onset of metal allergy[45,46]. Furthermore, the intake of sensitizer metals through food is an important cause[47]. Considering our results together with this information, metal nanoparticles could play an important role as sensitizers in these situations. Of course, we should also pay attention to the continuing prevalence of nanotechnology in our lives. We believe that further study to elucidate the contribution of metal nanoparticles to the onset of human metal allergy will help in the prevention of metal allergy.

Methods

Methods and any associated references are available in the online version of the paper.

Received 10 February 2015; accepted 27 April 2016; published online 30 May 2016

References

1. Thyssen, J. P., Linneberg, A., Menne, T. & Johansen, J. D. The epidemiology of contact allergy in the general population—prevalence and main findings. *Contact Dermatitis* **57,** 287–299 (2007).
2. Thyssen, J. P. & Menne, T. Metal allergy—a review on exposures, penetration, genetics, prevalence, and clinical implications. *Chem. Res. Toxicol.* **23,** 309–318 (2010).
3. Davis, M. D. *et al.* Patch testing with a large series of metal allergens: findings from more than 1,000 patients in one decade at Mayo Clinic. *Dermatitis* **22,** 256–271 (2011).
4. Richardson, C., Hamann, C. R., Hamann, D. & Thyssen, J. P. Mobile phone dermatitis in children and adults: a review of the literature. *Pediatr. Allergy Immunol. Pulmonol.* **27,** 60–69 (2014).
5. Rothenberg, M. E. Innate sensing of nickel. *Nature Immunol.* **11,** 781–782 (2010).
6. Lu, L. *et al.* Components of the ligand for a Ni^{++} reactive human T cell clone. *J. Exp. Med.* **197,** 567–574 (2003).
7. Gamerdinger, K. *et al.* A new type of metal recognition by human T cells: contact residues for peptide-independent bridging of T cell receptor and major histocompatibility complex by nickel. *J. Exp. Med.* **197,** 1345–1353 (2003).
8. Kimber, I., Bentley, A. N. & Hilton, J. Contact sensitization of mice to nickel sulphate and potassium dichromate. *Contact Dermatitis* **23,** 325–330 (1990).
9. Vreeburg, K. J., de Groot, K., van Hoogstraten, I. M., von Blomberg, B. M. & Scheper, R. J. Successful induction of allergic contact dermatitis to mercury and chromium in mice. *Int. Arch. Allergy Appl. Immunol.* **96,** 179–183 (1991).
10. Schmidt, M. *et al.* Crucial role for human Toll-like receptor 4 in the development of contact allergy to nickel. *Nature Immunol.* **11,** 814–819 (2010).
11. Artik, S., von Vultee, C., Gleichmann, E., Schwarz, T. & Griem, P. Nickel allergy in mice: enhanced sensitization capacity of nickel at higher oxidation states. *J. Immunol.* **163,** 1143–1152 (1999).
12. Sato, N. *et al.* Lipopolysaccharide promotes and augments metal allergies in mice, dependent on innate immunity and histidine decarboxylase. *Clin. Exp. Allergy* **37,** 743–751 (2007).
13. Johansen, P., Wackerle-Men, Y., Senti, G. & Kundig, T. M. Nickel sensitisation in mice: a critical appraisal. *J. Dermatol. Sci.* **58,** 186–192 (2010).
14. Wiesner, M. R. *et al.* Meditations on the ubiquity and mutability of nano-sized materials in the environment. *ACS Nano* **5,** 8466–8470 (2011).
15. Billi, F. & Campbell, P. Nanotoxicology of metal wear particles in total joint arthroplasty: a review of current concepts. *J. Appl. Biomater. Biomech.* **8,** 1–6 (2010).
16. Polyzois, I., Nikolopoulos, D., Michos, I., Patsouris, E. & Theocharis, S. Local and systemic toxicity of nanoscale debris particles in total hip arthroplasty. *J. Appl. Toxicol.* **32,** 255–269 (2012).
17. Thomas, P. *et al.* Increased metal allergy in patients with failed metal-on-metal hip arthroplasty and peri-implant T-lymphocytic inflammation. *Allergy* **64,** 1157–1165 (2009).
18. Glover, R. D., Miller, J. M. & Hutchison, J. E. Generation of metal nanoparticles from silver and copper objects: nanoparticle dynamics on surfaces and potential sources of nanoparticles in the environment. *ACS Nano* **5,** 8950–8957 (2011).

19. Mortensen, L. J., Oberdorster, G., Pentland, A. P. & Delouise, L. A. *In vivo* skin penetration of quantum dot nanoparticles in the murine model: the effect of UVR. *Nano Lett.* **8,** 2779–2787 (2008).
20. Rancan, F. *et al.* Skin penetration and cellular uptake of amorphous silica nanoparticles with variable size, surface functionalization, and colloidal stability. *ACS Nano* **6,** 6829–6842 (2012).
21. Liu, J., Sonshine, D. A., Shervani, S. & Hurt, R. H. Controlled release of biologically active silver from nanosilver surfaces. *ACS Nano* **4,** 6903–6913 (2010).
22. Askenase, P. W. Yes T cells, but three different T cells (alphabeta, gammadelta and NK T cells), and also B-1 cells mediate contact sensitivity. *Clin. Exp. Immunol.* **125,** 345–350 (2001).
23. Tsuji, R. F. *et al.* B cell-dependent T cell responses: IgM antibodies are required to elicit contact sensitivity. *J. Exp. Med.* **196,** 1277–1290 (2002).
24. O'Leary, J. G., Goodarzi, M., Drayton, D. L. & von Andrian, U. H. T cell- and B cell-independent adaptive immunity mediated by natural killer cells. *Nature Immunol.* **7,** 507–516 (2006).
25. Robbiani, D. F. *et al.* The leukotriene C(4) transporter MRP1 regulates CCL19 (MIP-3beta, ELC)-dependent mobilization of dendritic cells to lymph nodes. *Cell* **103,** 757–768 (2000).
26. Sixt, M. *et al.* The conduit system transports soluble antigens from the afferent lymph to resident dendritic cells in the T cell area of the lymph node. *Immunity* **22,** 19–29 (2005).
27. Itano, A. A. & Jenkins, M. K. Antigen presentation to naive CD4 T cells in the lymph node. *Nature Immunol.* **4,** 733–739 (2003).
28. Reddy, S. T., Rehor, A., Schmoekel, H. G., Hubbell, J. A. & Swartz, M. A. *In vivo* targeting of dendritic cells in lymph nodes with poly(propylene sulfide) nanoparticles. *J. Control. Release* **112,** 26–34 (2006).
29. Reddy, S. T. *et al.* Exploiting lymphatic transport and complement activation in nanoparticle vaccines. *Nature Biotechnol.* **25,** 1159–1164 (2007).
30. Moulon, C., Vollmer, J. & Weltzien, H. U. Characterization of processing requirements and metal cross-reactivities in T cell clones from patients with allergic contact dermatitis to nickel. *Eur. J. Immunol.* **25,** 3308–3315 (1995).
31. Kuroda, E., Coban, C. & Ishii, K. J. Particulate adjuvant and innate immunity: past achievements, present findings, and future prospects. *Int. Rev. Immunol.* **32,** 209–220 (2013).
32. Doorn, P. F. *et al.* Metal wear particle characterization from metal on metal total hip replacements: transmission electron microscopy study of periprosthetic tissues and isolated particles. *J. Biomed. Mater. Res.* **42,** 103–111 (1998).
33. Pacheco, K. A. Allergy to surgical implants. *J. Allergy Clin. Immunol. Pract.* **3,** 683–695 (2015).
34. Yin, Y., Liu, J. & Jiang, G. Sunlight-induced reduction of ionic Ag and Au to metallic nanoparticles by dissolved organic matter. *ACS Nano* **6,** 7910–7919 (2012).
35. Liu, J., Wang, Z., Liu, F. D., Kane, A. B. & Hurt, R. H. Chemical transformations of nanosilver in biological environments. *ACS Nano* **6,** 9887–9899 (2012).
36. Van der Zande, M. *et al.* Distribution, elimination, and toxicity of silver nanoparticles and silver ions in rats after 28-day oral exposure. *ACS Nano* **6,** 7427–7442 (2012).
37. Kaplan, D. H., Igyarto, B. Z. & Gaspari, A. A. Early immune events in the induction of allergic contact dermatitis. *Nature Rev. Immunol.* **12,** 114–124 (2012).
38. Rachmawati, D. *et al.* Transition metal sensing by Toll-like receptor-4: next to nickel, cobalt and palladium are potent human dendritic cell stimulators. *Contact Dermatitis* **68,** 331–338 (2013).
39. Cao, X. Self-regulation and cross-regulation of pattern-recognition receptor signalling in health and disease. *Nature Rev. Immunol.* **16,** 35–50 (2015).
40. Chen, G. Y. & Nunez, G. Sterile inflammation: sensing and reacting to damage. *Nature Rev. Immunol.* **10,** 826–837 (2010).
41. Pennino, D. *et al.* IL-17 amplifies human contact hypersensitivity by licensing hapten nonspecific Th1 cells to kill autologous keratinocytes. *J. Immunol.* **184,** 4880–4888 (2010).
42. Dyring-Andersen, B. *et al.* $CD4^+$ T cells producing interleukin (IL)-17, IL-22 and interferon-gamma are major effector T cells in nickel allergy. *Contact Dermatitis* **68,** 339–347 (2013).
43. Annunziato, F., Cosmi, L., Liotta, F., Maggi, E. & Romagnani, S. Human Th17 cells: are they different from murine Th17 cells? *Eur. J. Immunol.* **39,** 637–640 (2009).
44. Bachmann, M. F. & Jennings, G. T. Vaccine delivery: a matter of size, geometry, kinetics and molecular patterns. *Nature Rev. Immunol.* **10,** 787–796 (2010).
45. Mann, E. *et al.* Does airborne nickel exposure induce nickel sensitization? *Contact Dermatitis* **62,** 355–362 (2010).
46. Swinnen, I. & Goossens, A. An update on airborne contact dermatitis: 2007–2011. *Contact Dermatitis* **68,** 232–238 (2013).
47. Jensen, C. S., Menne, T. & Johansen, J. D. Systemic contact dermatitis after oral exposure to nickel: a review with a modified meta-analysis. *Contact Dermatitis* **54,** 79–86 (2006).

Acknowledgements

The authors thank Y. Morishita for supporting the evaluations of the physicochemical properties of nanoparticles. This study was supported by Grants-in-Aid for Scientific Research from the Ministry of Education, Culture, Sports, Science and Technology of Japan (MEXT) and from the Japan Society for the Promotion of Science (JSPS), by a Grant-in-Aid for JSPS Fellows, by Health Labour Sciences Research Grants from the Ministry of Health, Labour and Welfare of Japan (MHLW), by The Takeda Science Foundation, by The Research Foundation for Pharmaceutical Sciences, by The Japan Food Chemical Research Foundation, by the Urakami Foundation and by the Uehara Memorial Foundation.

Author contributions

T.Hi. and Y.Y. conceived and designed the experiments. T.Hi., N.I. and K.I. performed most of the experiments. T.Ha., N.N., E.U., K.S., H.T. and M.Y. helped with collecting tissue samples and splenocytes. T.Hi., Y.Y., N.I. and K.I. analysed the data. T.Hi. and Y.Y. wrote the manuscript. K.N., Y.M., H.K., S.T., K.J.I. and K.H. provided technical support and conceptual advice. Y.T. supervised all the projects. All authors discussed the results and commented on the manuscript.

Additional information

Supplementary information is available in the online version of the paper. Reprints and permissions information is available online at www.nature.com/reprints. Correspondence and requests for materials should be addressed to Y.Y. and Y.T.

Competing financial interests

Yasuo Yoshioka is employed by The Research Foundation for Microbial Diseases of Osaka University. All other authors declare no competing financial interests.

Methods

Nanoparticles and ions. Solutions of citrate-coated nAg5, nAg10, nAg50, nAg100 and nAu10 particles, as well as uncoated nNi3 particles, were purchased from nanoComposix in the form of stock dispersions (1 mg metal ml^{-1}) in aqueous 2 mM citrate (nAg5, nAg10, nAg50, nAg100 and nAu10) or in the form of stock powder (nNi3). nSP10 was purchased from Micromod Partikeltechnologie. Ag^+ (as $AgNO_3$) was purchased from Sigma-Aldrich and Ni^{2+} (as $NiCl_2$) was purchased from Wako. We confirmed the purity (>99.99%) of all the metal nanoparticles we used (nAg5, nAg10, nAg50, nAg100, nAu10 and nNi3) by elemental analysis using inductively coupled plasma mass spectrometry (ICP-MS). Elemental analysis was performed by the Japan Food Research Laboratories in Osaka, Japan.

Reagents. The anti-CD4 antibody (GK1.5) and anti-CD8 antibody (53-6.72) were purified from ascitic fluid collected from nude mice following transplantation of GK1.5 or 53-6.72 hybridoma cells (American Type Culture Collection). The anti-IFN-γ (R4-6A2), anti-IL-17A (TC11-18H10.1), rat IgG1, IgG2a and IgG2b for isotype control were purchased from BioLegend. Anti-asialo GM1 rabbit serum was purchased from Wako and the control rabbit serum was from Life Technologies. LPS (*Escherichia coli O55:B5*) was purchased from Sigma, and LPSa and ultrapure LPS (*E. coli O55:B5*) were purchased from InvivoGen (ultrapure grade).

Mice. Female BALB/c, BALB/c *nu/nu* and C57BL/6 mice were purchased from SLC and female C.B-17 SCID mice were purchased from Charles River Japan. All mice were used at 6 to 10 weeks of age. All animal experiments were performed in accordance with the institutional guidelines of Osaka University and the National Institute of Biomedical Innovation for the ethical treatment of animals.

Sample preparation for treatment. For injection to mice, all metal solutions for sample injection were diluted to 0.8 mg metal ml^{-1} in glucose solution (final conc. 5%, isotonic; Fuso) except the Ag^+ solution for injection to the ear for elicitation. The nSP10 particles were also diluted to 0.8 mg ml^{-1} in the same glucose solution. The concentration of Ag^+ used for sample injection to the ear for elicitation was 0.09 mg silver ml^{-1}. In most experiments, we used mixtures of each solution and LPS (final conc. 10 μg ml^{-1}). These solutions were prepared immediately before use.

Ag or Au release in samples. Solutions of 1 μg ml^{-1} nAg or nAu (immediately after preparation in water or after storage in RPMI 1640 (Wako) supplemented with 10% fetal bovine serum, 10 ml l^{-1} of a 100× nonessential amino acid solution (Gibco, Invitrogen), 50 μM 2-mercaptoethanol (Gibco) and 1% antibiotic cocktail (10,000 U ml^{-1} penicillin, 10,000 μg ml^{-1} streptomycin, 25 μg ml^{-1} amphotericin B; Gibco) for 24 h at 37 °C were centrifuged (2 h, 40,000*g*, 4 °C). The supernatant was collected and the amount of Ag or Au in the supernatant was determined by ICP-MS.

Physicochemical examination of nanoparticles. nAg was diluted to 0.05 mg ml^{-1} with 5% glucose, and the mean particle diameter was measured using a Zetasizer Nano ZS (Malvern Instruments). Specifically, the mean diameters of the nanoparticles were measured by means of a dynamic light-scattering method. Measurements were performed using capillary cells (Malvern Instruments). The size and shape of the nanoparticles were observed using TEM. The nanoparticles were placed on 200-mesh carbon-coated copper TEM grids (Nissin EM) and observed by TEM (H-7650; Hitachi High-Technologies Corporation).

Analysis of sensitization potentials of metal nanoparticles. Mice were injected with each type of metal nanoparticle or metal ions (0.8 mg metal ml^{-1}) with LPS (10 μg ml^{-1}) to both footpads at a rate of 20 μl per footpad every week for 4 weeks. One week after the final injection, the mice were intradermally administered with 10 μl metal solutions (0.8 mg metal ml^{-1} or 0.09 mg Ag^+ ml^{-1}) on their right ear, and 10 μl of vehicles for the metal solutions was injected into their left ear. We measured ear thickness using a dial thickness gauge (0.001 mm type; Ozaki Mfg. Co.) at 24, 48, 72 and 96 h post-injection. The metal-induced ear swelling is expressed as the right ear swelling minus the left ear swelling.

Histological analysis. Ninety-six hours after injection, the ears of the mice were removed and placed in a fixative solution (4% paraformaldehyde in PBS; Wako). The ears were embedded in paraffin blocks and sliced. The ear sections were stained with haematoxylin and eosin. Histopathological examination was performed by the Applied Medical Research Laboratory. The number of total inflammatory cells (lymphocytes, granulocytes and monocytes) in two high-power fields (×400 magnification) selected at random from the sample injection site was measured by a researcher who was unaware of the treatment assignments.

***In vivo* cell depletion experiment.** For cell depletion experiments, the nAg10-sensitized mice were treated intraperitoneally with 500 μg per mouse of anti-CD4 antibody or rat IgG2b isotype control, or anti-CD8 antibody or IgG2a isotype control in PBS, or intravenously with 50 μl per mouse of anti-asialo GM1 rabbit serum or control rabbit serum 24 h before injection of nAg10 to the right ear of each mouse. Cell depletion was determined by means of flow cytometry ($CD4^+$ cells and $CD8^+$ cells >95% depletion, NK cells; $CD3^-$, $CD49b^+$ cells >80% depletion in splenocytes 96 h after challenge).

Serum transfer experiments. For serum transfer experiments, 'donor' mice were injected weekly with nAg10 or vehicles and LPS on their footpads for 4 weeks. One week after the last injection, the blood of the nAg10-sensitized 'donor' mice was sampled by cardiac puncture. These blood samples were incubated for 1 h at 37 °C and additionally for 5 h at 4 °C. After incubation, the blood samples were centrifuged at 5,000*g* at 4 °C for 15 min to obtain the serum. Immediately after serum collection, two to three serum samples were pooled and then the non-treated 'recipient' mice (9–10 weeks old) were injected intraperitoneally with 500 μl of the pooled serum. At 24 h after the transfer, the recipient mice were injected with nAg10 in their right ear and with nAg10 vehicles in their left ear.

$CD4^+$ T cells transfer experiments. For $CD4^+$ T cell transfer experiments, 'donor' mice were injected weekly with nAg10 and LPS on their footpads for 4 weeks. A pooled single-cell suspension was prepared from three or four donor mouse spleens and popliteal lymph nodes 1 week after the last injection. $CD4^+$ T cells were negatively isolated with a $CD4^+$ T cell isolation kit (Miltenyi Biotec) according to the manufacturer's instructions. $CD4^+$ T cell purity was determined by flow cytometry ($CD3^+$, $CD4^+$ cells >95% purification). Immediately after cell preparation, 2×10^7 $CD4^+$ T cells were injected intravenously into non-treated 'recipient' mice (9–10 weeks old). At 24 h after transfer, the recipient mice were injected with nAg10 in their right ear and with nAg10 vehicles in their left ear.

Effector cytokine responses. Splenocytes (1×10^6 cells per well) from mice that were injected weekly with nAg10 or nNi3 and LPS on their footpads for 4 weeks were re-stimulated with each nanoparticle or with ions. After incubation of the cells for 72 h, the levels of IL-4, IL-5, IL-9, IL-13, IL-17A and IFN-γ in the supernatants were measured by enzyme-linked immunosorbent assay (IL-4, IL-5, IL-9, IL-13, IL-17A, eBioscience; IFN-γ, BD Biosciences) according to the manufacturer's instructions. Cell viability was determined by using a WST-8 assay kit (Nacalai Tesque).

Cytokine analysis by real-time PCR. Ear samples were collected at 24, 48 and 96 h post-injection of nAg10, and footpad samples were collected at 4 h post-injection of LPS with each size of nAg. These samples were stored in RNAlater (Qiagen) at 4 °C for 24 h and then at −20 °C until analysis according to the manufacturer's instructions. Total RNA was extracted from the samples using an RNeasy Mini Kit (Qiagen) according to the manufacturer's instructions and then reverse-transcribed to complementary DNA (cDNA) using a SuperScript VILO cDNA Synthesis kit (Invitrogen) according to the manufacturer's instructions. Real-time PCR was performed using TaqMan Gene Expression Assays (Life Technologies; *Il17a*: Mm00439619_m1, *Il6*: Mm00446190_m1 and *TNFα*: Mm00443258_m1) and the StepOnePlus Real-Time PCR system (Life Technologies) according to the manufacturer's instructions. The threshold cycle (CT) values were determined using the default settings. All real-time PCR reactions were run in triplicate, and average CT and standard deviation values were calculated. The expression of mRNA was normalized to the expression of *GAPDH* mRNA (encoding glyceraldehyde phosphate dehydrogenase) by the change in cycling threshold (ΔCT) method and calculated based on $2^{-\Delta\Delta CT}$.

Cytokine blockade experiments. nAg10-sensitized mice were injected weekly with nAg10 and LPS on their footpads for 4 weeks and were then treated intraperitoneally with 500 μg mouse of anti-IFN-γ antibody or rat IgG1 isotype control in PBS, or were treated intravenously with 200 μg mouse of anti-IL-17A antibody or rat IgG1 isotype control in PBS on the day of sample injection into the right ear.

Sample preparation *in vivo* for ICP-MS. The mice were injected with each silver sample in their right ear. At 24, 48 and 96 h, right ear lymph nodes were collected and 1 ml nitric acid and 1 ml hydrogen peroxide were added. The samples then underwent microwave digestion (ETHOS One, Milestone General). The obtained solutions were diluted with distilled water to 10 ml. The solutions were diluted with ~10% nitric acid. These sample preparations for ICP-MS were performed by the Japan Food Research Laboratories.

ICP-MS. Elemental Ag was measured by ICP-MS (Agilent 7700x ICP-MS, Agilent Technologies). The main instrumental operating conditions were as follows: RF power, 1,550 W; carrier gas flow, 1.05 l Ar min^{-1}. The following isotopes were measured: ^{107}Ag, ^{197}Au, ^{103}Rh and ^{205}Ti. Samples with measured concentrations below the lowest determination level were counted as 0 ng ml^{-1}. The lowest determination level was 20 pg ml^{-1}. Before ICP-MS measurement, aliquots were spiked with the internal standard ^{103}Rh (for Ag) or ^{205}Ti (for Au) to achieve an internal standard concentration of 2 ng ml^{-1}. Quantification was carried out by external six-to-nine-point calibration with internal standard correction.

TEM analysis of dLNs. The mice were injected with each silver sample in their right ear. At 24 h post-injection, the whole body of each mouse was perfused with a mixture of 2% glutaraldehyde and 2% paraformaldehyde in phosphate buffer, then right ear dLNs were collected and additionally fixed in a mixture of 2% glutaraldehyde and 2% paraformaldehyde for 24 h. The samples were then washed

with phosphate buffer three times and post-fixed in sodium cacodylate-buffered 1.5% osmium tetroxide for 60 min at 4 °C, block stained in 0.5% uranyl acetate, dehydrated by dipping each sample in a series of ethanol solutions containing increasing concentrations of ethanol and embedded in Epon resin (TAAB Laboratories Equipment). Ultrathin sections were stained with uranyl acetate and then with lead citrate (TAAB Laboratories Equipment). The stained samples were subsequently observed under TEM (Hitachi H-7650). TEM analysis of dLNs was performed by the Laboratory of Common Apparatus at the National Institute of Biomedical Innovation in Osaka.

Statistical analysis. Statistical analyses were performed with Ekuseru-Toukei 2012 software (Social Survey Research Information Co.). All data are presented as means ± s.e.m. Significant differences between control groups and experimental groups were determined using Dunnett's test. $P < 0.05$ was considered significant. We did not use any statistical method to determine the sample size in the experiments. The sample size in each experiment was determined empirically for sufficient statistical power. We did not use any randomization methods. The investigators were not blinded to group allocation during experiments and analyses except for the histological analysis.